ITTC Quality System Manual

Recommended Procedures and Guidelines

Guideline

Uncertainty Analysis for Model Testing of Offshore Wind Turbines

7.5	Process control
7.5-02	Testing and Extrapolation Methods
7.5-02-07	Loads and Responses
7.5-02-07-03	Ocean Engineering
7.5-02-07-03.17	Uncertainty Analysis for Model Testing of Offshore Wind Turbines

Disclaimer

Updated / Edited by	Approved
Specialist Committee on Ocean Renewable Energy of the 30th ITTC	30th ITTC 2024
Date: 05/2024	Date: 09/2024

Table of Contents

Uncertainty Analysis for Model Testing of Offshore Wind Turbines

1. PURPOSE OF THIS GUIDELINE

The purpose of the guideline is to provide guidance on the application of uncertainty analysis to the model scale testing of offshore wind turbines following the ITTC Procedure 7.5-02-07-03.8, “Model Tests for Offshore Wind Turbines”. The model scale testing of offshore wind turbines focuses on the environmental loads and global response of the structure, similar to the testing of other offshore structures (floating or fixed).

The uncertainty analysis should be performed following the ITTC Procedures 7.5-02-01-01, “Guide to the Expression of Uncertainty in Experimental Hydrodynamics” (ITTC 2014a), 7.5-02-02-02, “General Guidelines for Uncertainty Analysis in Resistance Tests” (ITTC 2014b), and 7.5-02-01-07, "Guideline to Practical Implementation of Uncertainty Analysis" (ITTC 2017a). These guidelines are based on the comprehensive International Organization for Standardization (ISO) Guide to the Expression of Uncertainty in Measurement (JCGM, 2008a), also referred to as GUM. The following procedure adapts the same notation and definitions as provided in ITTC Procedure 7.5-02-01-01 "Guide to Expression of Uncertainty in Experimental Hydrodynamics" (ITTC2014a).

2. GENERAL GUIDE TO UNCERTAINTY ANALYSIS

The aim of an uncertainty analysis is to provide a quantitative measure of how reliable (or to what level of precision) a measurement is. According to the GUM uncertainty framework (JCGM, 2008a), the uncertainty of a measurement can be defined as the "parameter, associated with the result of a measurement, that characterizes the dispersion of the values that could reasonably be attributed to the measurand."

The GUM uses the following definitions when describing uncertainties: standard uncertainty, combined standard uncertainty, and expanded standard uncertainty.

2.1 Standard uncertainty

The standard uncertainty (u) is the uncertainty of the result of a measurement expressed in terms of a standard deviation. The standard uncertainty can be grouped into two types, Type A and Type B, where the type depends on the method for estimation of uncertainty.

In the following a brief description of the two types of uncertainty is given, for further info please refer to the Procedure 7.5-02-01-01 Guide to the Expression of Uncertainty in Experimental Hydrodynamics.

Type A: Uncertainty components obtained using a method based on statistical analysis of a series of observations. The standard uncertainty by Type A for a series of n repeated samples (or observations) is estimated by:

$$u(\bar{q}) = s/\sqrt{n} \tag{1}$$

where s and $\bar{q}$ are the standard deviation and arithmetic mean, respectively, of the samples.

Type B: Uncertainty component obtained by other means (other than statistical analysis). Prior experience and professional judgements are part of Type B uncertainties.

2.2 Combined standard uncertainty

If a measurement result y is obtained from N other measured quantities $x_1, x_2, \ldots, x_N$, then the standard uncertainty of the result is a combination of the standard uncertainties of the other quantities. This combined standard uncertainty u_c is given by the law of propagation of uncertainty. I.e. for a measurement result $y=f(x_1,x_2,\ldots,x_N)$, the combined standard uncertainty is defined as:

$$u_c^2(y) = \sum_{i=1}^{N} c_i^2 u^2(x_i) + 2\sum_{i=1}^{N-1}\sum_{j=i+1}^{N} c_i c_j u(x_i) u(x_j) r(x_i, x_j) \tag{2}$$

where the sensitivity coefficients $c_i = \partial f/\partial x_i$ and $c_j = \partial f/\partial x_j$ determines how the measurement result varies with changes in these quantities. Furthermore, $r(x_i,x_j)$ is the correlation coefficient and ranges between -1 and +1. If the input quantities x_i and x_j are uncorrelated, then $r(x_i,x_j)=0$ and the combined standard uncertainty equation (2) reduces to the first summation term only.

2.3 Expanded standard uncertainty (U)

The expanded standard uncertainty $U=ku_c(y)$ is introduced to provide an interval about the measurement result that may be expected to encompass a large fraction of the distribution of values which could reasonably be attributed to the measurand Y. The numerical value for the coverage factor k should be chosen so that the interval $Y = y \pm U$ corresponds to a particular level of confidence. This factor usually corresponds to 95% confidence.

For most hydrodynamic towing tank or wave basin experiments, the Student t-distribution may be assumed for a small number of observations (cf. Figure 1 in ITTC, 2014a). For a large number of degrees of freedom ($\upsilon = n$-1>30), the distribution may be assumed to be Gaussian with a coverage factor of k=1.960.

2.4 The GUM approach for evaluating and expressing uncertainty

The evaluation and expression of uncertainty can be achieved by following the procedures outlined in the GUM uncertainty framework (JCGM, 2008a, Sect. 8), which are also summarized in ITTC Procedure 7.5-02-01-01, titled "Guide to the Expression of Uncertainty in Experimental Hydrodynamics" (ITTC 2014a). It is based on a Taylor series expansion of the model equation $y=f(x_1,x_2,\ldots,x_N)$.

2.5 Limitations with the GUM approach

The GUM approach is based on using the law of propagation of uncertainties and relies on the following assumptions:

1. Linearization: The model for calculating the measurand must have insignificant nonlinearity.
2. Central limit theorem: The probability distribution of the output is approximately normal and can be represented by a t-distribution.
3. Welch-Satterthwaite formula can be used for the evaluation of the effective degrees of freedom, to calculate expanded standard uncertainty.

These assumptions may not be valid if the problem is strongly nonlinear and/or the resulting distribution is asymmetric, violating the validity of the central limit theorem approach. Also, the Welch-Satterthwaite formula for calculating the effective degrees of freedom may not always be adequate for the problem considered.

Note that nonlinearities can be addressed by incorporating higher-order derivatives in Equation (2). This requires that the model function *f* is continuously differentiable up to the appropriate order.

It is only expectation and standard deviations that is propagated in the GUM approach (see Figure 1).

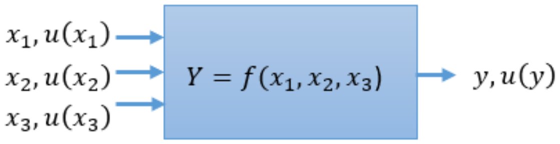

Figure 1 Illustration of propagation of uncertainties

2.6 The Monte Carlo approach

The GUM Supplement 1 (JCGM, 2008b) presents an alternative method for cases when the classical GUM approach fails, based on Monte Carlo simulations.

Monte Carlo simulations generate numerous model variations by randomly sampling input variables from their probability distribution. Each scenario is then simulated, and the resulting outcomes can be utilized to establish a probability distribution of possible results.

The Monte Carlo method overcomes the limitations of the GUM approach with nonlinearities and asymmetric outcomes. It propagates the entire probability distributions of the input quantities x_i (see Figure 2) and is therefore said to provide results that are closer to reality compared to the simpler law of propagation of uncertainties (Couto et al., 2013).

Possible disadvantages of the Monte Carlo approach are:

1. Computational intensity: it may require a large computational cost if the underlying model is complex.
2. Efficiency: when considering many response functions, this method may not be the most efficient

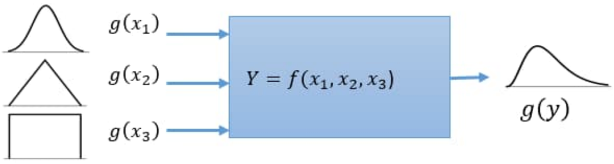

Figure 2 Illustration of propagation of distributions

3. SOURCES OF UNCERTAINTY FOR TESTING OFFSHORE WIND TURBINES

A first step in uncertainty analysis is to identify all significant sources of uncertainty. The sources of uncertainty related to model testing of offshore wind turbines can be grouped into these main blocks: model, installation, control system and actuators, measurement and data processing, environmental condition modelling, and initial test conditions.

In the following sections the various sources of uncertainties are discussed, and a summary is provided in Table 1. Unless specified, each source should be considered relevant both for fixed and floating offshore wind turbines.

Table 1: Uncertainty categories and sources

Categories	Sources	Examples (related to all sources)
Model	Rotor nacelle assembly, tower, and substructure Stationkeeping system (only floating) Foundation (only bottom-fixed) Numerical model (if applicable)	Mass properties, geometry, structural elasticity Restoring forces "Soil" stiffness and damping Numerical approximation
Model installation	Ballasting and trimming (only floating) Positioning and alignment	Reading of trimming
Control systems and actuators	Variable speed control Blade pitch control Actuators Hybrid testing (if applicable)	Tip-speed ratio Blade pitch angle Achievement of target aerodynamic loads
Measurement and data processing	Measurement sensors Test duration and realization of extreme events Data acquisition Postprocessing	Accuracy Precision
Environmental condition modelling	Non-controlled physical properties Waves Wind Current	Temperature, density, viscosity Wave spectra Wind spectra Current turbulence
Initial test conditions	Mooring lines (only floating) Time between two consecutive tests	Mooring layout Remaining turbulence and fluid circulation
Other	Scaling effects	Reynolds vs Froude scaling Viscous forces due to limitations with Reynolds number

3.1 Model

Uncertainty sources related to the model (the test object) are mainly a result of tolerances in manufacturing and deformation occurred after manufacturing (e.g., during installation and model testing). These steps create uncertainties in the model geometry, the inertial properties, and structural elasticity and damping. Furthermore, if numerical simulations are necessary to prepare or perform the experiments, there will be sources of uncertainties associated with the numerical model.

Offshore wind turbines usually comprise of the following parts: The rotor and nacelle assembly (RNA), tower, substructure (floating or bottom-fixed), station keeping system (floating) or sea-bed foundation (bottom-fixed).

Uncertainty sources related to the model are outlined below.

3.1.1 Rotor nacelle assembly and tower

The rotor nacelle assembly (RNA) represents a considerable source of uncertainty (Robertson, 2017). The blade geometry, pitch setting, mass distribution, structural damping and stiffness are the most significant sources. Manufacture of a rotor with the correct mass properties and adequate stiffness can prove very challenging. The complexity of the blade geometry and its influence on the turbine loading represent a significant uncertainty in the measured loads from the definition of the RNA model.

The tower stiffness, structural damping, mass distribution, and its connection to the RNA and substructure represent other sources of uncertainty. The tower is often connected to the RNA and substructure through load cells. This may add additional compliance to the system and is another source of uncertainty.

For a fully instrumented physical rotor model, it may also be difficult to achieve the scaled-down mass (Gueydon, 2016), especially for smaller model scales. This can be accounted for by shifting masses in the support structure to maintain the global moments of inertia and centre of gravity (COG), but the mass distribution will not be maintained which is of importance for force measurements and structural modes for elastic towers.

3.1.2 Substructure

Uncertainties in the substructure will come from the geometry, mass distribution and stiffness properties. Distortion of geometry may affect the displaced volume and waterplane area, both affecting the hydrostatic properties and hydrodynamic loading. Furthermore, the surface roughness and sharp/rounded corners/edges may affect viscous damping.

Uncertainty in the mass distribution affects the inertia properties of the floater as well as the centre of mass. Stiffness properties of flexible members and joints may also be a source of uncertainty.

Small water absorption or deformation due to hydrostatic pressure can influence the model draught and mass distribution, being another source of uncertainty.

3.1.3 Station keeping system

The purpose of a station keeping system is to limit the horizontal excursions and maintain orientation of floating wind turbines. The type of station keeping system depends on the type of floater, and typically it comprises of mooring lines and anchors, tendons anchored to sea bottom, and/or active thrusters (DP-system). The latter is less relevant for offshore wind turbines.

As for mooring lines and tendons it is important to maintain the correct line characteristics. Uncertainties relate especially to the difficulty of scaling the axial stiffness (EA) distribution and the mass distribution at the same time (Qiu et al., 2014). This often leads to partial or total replacement of original segments with additional spring elements, and clump weights and/or buoyance elements to correct submerged weight.

Other sources of uncertainty that influence the line characteristics include fairlead position, line segments length and diameter, line pretension, anchor positions, and sea-bottom friction. In-line load cells used to measure line tension may also alter the properties of the lines and tendons.

In the case where it is required to model a mooring system consisting of synthetic fibre ropes, the large sensitivity to extreme mooring loads of the material should be considered to correctly reproduce the stress-strain characteristics. Dynamic characteristics of the synthetic ropes should also be considered.

Truncation or other simplifications of the mooring lines may lead to other distortions, and in some cases to a totally different mooring system than originally specified (Qiu et al., 2014). It is important to maintain correct geometrical parameters such as top angles and lines elongation during excursion. Uncertainty analysis should be conducted to determine the degree to which the restoring characteristics have been achieved and to allow this effect to be included in an analysis of the overall model test.

3.1.4 Foundation

For bottom-fixed wind turbines, the soil stiffness and damping cannot be neglected due to its influence on the global response. Typically, the foundation is modelled by a "soil spring" extended down to the foundation. This connection should be designed to give realistic stiffness, but also damping for cases when aerodynamic damping is low. The imperfection and/or simplification of the soil model is a source of uncertainty.

The bottom stiffness may also be an uncertainty if the foundation is not rigidly fixed to the ground. The force transducer at the base of the wind turbine may also alter the stiffness of the foundation as well.

3.1.5 Numerical model

Numerical simulation models may constitute an important part of a test object, either in redesign of the model due to limitations when scaling down the structure (e.g., performance scaling of rotor blades, truncation of mooring lines) or as a replacement of a physical substructure by numerical simulations and actuators (e.g., hybrid testing).

Sources of uncertainties in the numerical modelling can be caused by, e.g., choice of mathematical model to describe real physics, introduction of empirical parameters, choice of numerical method, grid and timestep resolution, numerical accuracy and convergence criteria, computing capacity and simulation time, among others.

3.2 Model installation

Installation uncertainty sources relate to hull model ballasting and trimming, model positioning and alignment relative to wave maker and wind generator, mooring and anchor layout (including mooring line pretension and top angle), fastening of bottom fixed structures, and so forth.

Another source of installation uncertainty may relate to deformation of the model due to brute force from manual labour when moving or fixing the model.

3.3 Control systems and actuators

There are model parameters necessary for control design to ensure that the controller does not introduce any destabilizing dynamic system behaviour that would lead to excessive and unrealistic loads above rated operating conditions: aerodynamic coefficients (power and thrust), drivetrain mass, inertia, platform surge/pitch eigenfrequencies, platform surge/pitch damping, platform mass/inertia, platform hydrodynamic coefficients, quasi-static mooring lines, wind turbine mass/inertia, tower elasticity, blade elasticity, blade polars, yawed inflow, aeroelastic stability, 3D gyroscopic effects, and others.

3.3.1 Variable speed control

From cut-in wind speed to rated wind speed the rotor speed varies to allow for an optimal power production. Thus, the optimal tip-speed ratio TSR is tracked by controlling the rotor speed Ω with the generator torque at all operating wind speeds v_0: $TSR=\Omega R/v_0$. No negative damping effect arises for below-rated wind speeds since the thrust is increasing with increasing wind (Jonkman 2007). For variable speed control, the uncertainty relates to the actual rotor speed Ω.

3.3.2 Blade pitch controller

The most critical control region is the region above rated wind speeds, where the collective blade pitch controller is active to keep the generator torque and rotor speed constant. A PI-controller is usually adopted. The dynamics including the controller and the closed feedback loop of rotor speed to blade pitch angle is referred to as "closed-loop dynamics". In order to keep the closed-loop system dynamics constant throughout all operating points above rated conditions, a method called "gain scheduling" is necessary. For floating wind turbines, this above-rated control is especially critical since the pitching of the blades can destabilize the floating wind turbine system. Uncertainty analysis should be conducted on the gain scheduling to determine the degree to which the target blade pitch angle has been achieved.

3.3.3 Required actuators

The actuators for modern wind turbines control the three blade-pitch angles and the generator torque. The blade pitch actuators can be independent of each other to allow for individual pitch control (IPC). This accounts for azimuth-dependent wind loads and reduces the blade and tower-top fatigue loads. Usually, a brushless motor is used to control the turbine rotation speed and torque in water basin model tests. The driving torque is measured by a torque sensor. The Type B uncertainty of motors and torque meters is estimated by the manufacturer's specifications.

3.3.4 Hybrid testing

In hybrid testing where the aerodynamic loads on the blades are simulated and imposed by actuators or a passive mass or a disc, uncertainty analysis should be conducted as per ITTC recommended Procedure (7.5-02-01-01, Guide to Expression of Uncertainty in Experimental Hydrodynamics) to determine the degree to which the target wind load characteristics have been achieved and to allow this effect to be included in an analysis of the overall model test.

3.4 Measurement and data processing

Wave, current, wind, model motions, rotor speed, generator speed, shaft torque, generator torque, power, bending moments, accelerations, and relative motions, etc. are the primary measurements in water basin model tests. All parameters are subjected to Type A and Type B uncertainties. Type A uncertainty is evaluated based on repeated measurements and Type B uncertainty is not revealed by repetition of the experiment. Type B sources of uncertainty include the geometry of used models, measurement sensors, the calibration and installation of equipment, data acquisition systems, data processing, etc.

3.4.1 Measurement sensors

It is very important to ensure that the instrumentation used in the test set-up have the required properties. Common sensors mainly used for measurement are the followings: Real-time optical tracking system, loadcell (i.e., 6-axis, one-axis, ring-type, etc.), torque meter, mooring line tension meter, wave probe, anemometer, current speed meter, thermometer, accelerometer, pressure gauge, strain gauge, inclinometer, leveller, electric weight scale, linear variable differential transformer (LVDT), electric current meter, etc. Specifications provided by sensor manufacturers and previous experience with sensors allow for the estimate of Type B uncertainties.

Sensors are often affected by the temperature. For slow variations in temperature this can introduce drift in the measured signal. This can be controlled by making a zero reading. When a pressure gauge hits the water, the temperature changes abruptly due to the difference in air and water temperature. Temperature change occurs at the same time as the impact pressure changes and thus direct use of the measured signal can give totally misleading results (Steen, 2014).

Careful calibration procedures are important to minimize measurement uncertainty. Generally, in-situ end-to-end calibration includes as many elemental uncertainty sources in the system as possible which do not have to be identified or individually estimated. Also, calibration standard, calibration misalignments, calibration curve fitting and A/D conversion are considered in the estimate of uncertainty. The curve fitting uncertainty can be estimated using the standard deviation of estimate formula. (ITTC procedure 7.5-02 07-02.1 Rev.4, 2011) The Type B uncertainty of A/D conversion is equal to half of resultant resolution.

Some measurements require the presence of cables attached to the RNA, and these may be a source of uncertainty for the mass, moments of inertia, aerodynamic loads, and damping. Careful calibration methodology must be followed to properly quantify the effect of the cables (e.g., decay test with and without cables).

3.4.2 Time duration and realization of extreme events

Realizations of combined environments in water basins require different time durations for load cases to be stochastically valid: 10 minutes under wind and regular waves for effective RAOs, 1 hour under wind and irregular waves for operating conditions, or 3 hours under wind and irregular waves for extreme events with initial transient periods. All the time durations above are in full scale. Specially, the properties of short and steep waves may change downstream, and the wave measurements should be carried out along the entire test track during wave calibration. Also, the shape of the irregular wave spectrum is an important uncertainty source, and it is required to ensure the measured spectrum shape agrees with the theoretical shape.

Due to limitations of the numerical simulation and/or ocean basins, different combinations of durations and number of seeds are used for the wind and wave realizations. The uncertainty of the wind and wave extreme values depends on the selected approach.

3.4.3 Data acquisition

A typical data acquisition system consists of a signal conditioner, Analog-to-Digital Converters (ADCs), and computer bus. Signal conditioning includes amplifying, filtering, smoothing, etc. When in-situ end-to-end calibration procedure is applied, all the data acquisition system elemental uncertainty sources are included in the process except for the noise. Both sampling rate and bit resolution are considered in selecting ADC and its uncertainty can be estimated by processing a known signal with a known analytical solution (i.e., sine).

3.4.4 Postprocessing

Postprocessing includes collection of measured data, data filtering, digitization of analog signals including peaks, reduction to a non-dimensional format, regression on the test data to acquire a mathematical fit, calculation of RAOs, spectrum, exceedance probability, stochastic averages (probability density function, cumulative density function, joint probability density function, mean, standard deviation, significant value, etc.) and long-term prediction with 50 to 100 year extreme values using the generalized extreme values distribution (i.e. Gumbel & Weibull, etc.). The Type B uncertainty should be included.

3.5 Environmental condition modelling

The uncertainties associated with the environmental condition modelling are related to multiple sources: the physical properties of the testing environment (e.g., air and water temperature and density, bottom friction, etc.), and the physical properties of the generated environment characteristics (e.g., wind, waves, and currents).

3.5.1 Physical properties

Some of the environmental physical properties that are important sources of uncertainty but are not necessarily controlled are: air density and temperature, water density and temperature, ocean basin floor friction, and water depth.

These uncertainties are linked to the accuracy of the instruments used to measure them, and to their variability over the time and space scales of the test – which may require repeated measurement in different points (space scale) and at different times (time scale) to reduce the uncertainty.

If controlled (e.g., moving floor to achieve desired water depth), the limitations of the control system, such as accuracy and repeatability, constitute an additional source of uncertainty.

3.5.2 Waves

A second source of uncertainty is the temporal and spatial variability of the generated waves, and its significance is related to how well the used measuring system captures these variabilities.

From a temporal point of view, wave reflection may be a source of uncertainty, such as the reflections at wave-maker and at tank boundaries

From a spatial point of view, for example, if the water surface elevation is measured only in one or few points of the tank, uncertainty on the actual surface elevation in other points may arise. Guidelines on where to measure these characteristics are given in the ITTC Recommended Procedure 7.5-02-07-03.1 “Floating Offshore Platform Experiments” (ITTC 2017b). Another spatial uncertainty may be the wave kinematics variability with depth, if these characteristics are measured only at one water depth – this is even more important when shallow water conditions are present. Incorrect boundary conditions can also lead to low frequency parasitic waves which serve as an additional source of uncertainty.

Tests involving physical wind introduce another source of uncertainty on the waves. The wind may cause disturbances to the waves near the free surface, which can have an adverse effect on the experimental results.

Furthermore, a Type A source of uncertainty is related to the inherent stochasticity of irregular waves over time. Repeated measurements can reduce this source of uncertainty.

3.5.3 Wind

An important source of uncertainty originates from the limitations, in terms of accuracy and repeatability, of the physical equipment used to generate wind (for hybrid testing, where the wind is simulated numerically and only wind forces are generated physically, see section "Numerical model" below).

Similar to waves, important spatial and temporal variabilities characterize a generic turbulent wind acting on an offshore wind turbine model, and the magnitude of these uncertainties is linked to in how many points (spatial) and how often (temporal) a measurement of the wind speed is taken.

For example, from a spatial point of view, even measurements taken in multiple points across the wind rotor plane (2-D) would not capture the wind velocity and wind turbulence variability in a plane perpendicular to the rotor plane – which can be significant for a floating offshore wind turbine system, as noted by Robertson (2017). Wind-wave interaction and wind blockage are other sources of wind spatial and temporal variability.

The temporal variability of wind speed and turbulence may also be an important source of uncertainty.

Furthermore, a Type A source of uncertainty arises when testing in turbulent wind conditions, due to the inherent stochasticity of turbulence. Repeated measurements can reduce this uncertainty.

3.5.4 Current

The limitations, in terms of accuracy and repeatability, of the physical equipment used to generate the current is a primary source of uncertainty.

As for waves and wind, the impact of the spatial variability of current velocity and turbulence on uncertainty should be assessed by measurements made at multiple points, both across the horizontal plane and the vertical water column.

In addition, turbulent currents are inherently stochastic, leading to a Type A uncertainty. Repeated measurements can reduce this uncertainty.

3.5.5 Numerical model

As reported by the ITTC Recommended Procedure 7.5-02-07-03.8 "Model Tests for Offshore Wind Turbines" (ITTC, 2017c), hybrid testing refers to "methods that combine, in real time and interactively, the numerical simulation of a virtual substructure with a physical substructure tested experimentally in model scale."

As such, the additional uncertainty sources to be considered in this case are linked to two factors: the numerical simulation model, and the physical equipment used to "convert" the forces calculated numerically into physical forces acting on the physical substructure.

In every numerical simulation, the numerical model adopted is a simplification of the real phenomenon, and therefore a source of uncertainty is the accuracy with which the numerical model reproduces the physical phenomenon. Usually, the physical wind and forces acting on the rotor are emulated, respectively, by a synthetic (numerically generated) wind speed and a numerical aerodynamic model deriving the forces transmitted by the rotor to the wind turbine tower at model scale. Therefore, in this case, the uncertainty is linked to the accuracy of the numerical approaches used to reproduce the wind spatial (e.g., wind shear) and temporal (e.g., turbulence) variability, and to the accuracy of the numerical approach used to calculate the wind forces acting on the rotor. For example, the Blade Element-Momentum theory is usually used to calculate these aerodynamic forces, due to their relatively low computational cost, but these are known to have several limitations (see, for example, Gupta et al., 2005).

The forces calculated by the numerical simulation are then downscaled and imposed on the physical model through a physical system. Depending on the system (single ducted fan driven by an electronic motor, as in Azcona et al. (2014), or a set of fans as in Urban and Guanche (2019), or actuated cables as in Sauder et al (2016), Bachynski et al. (2016), and Berthelsen et al. (2016), among others), the sources of uncertainty are linked to the limitations (accuracy and repeatability) of the components used.

3.6 Initial test conditions

Initial mooring line configuration on the bottom (hysteresis) and water basins initial conditions (i.e., remaining waves, circulation, turbulence, current, etc.) are primary uncertainty sources of initial test set-up and the uncertainties are estimated by the past experiences.

Due to small asymmetries in the model arrangement, a small roll response may occur in head sea and this roll increases when the rotor is in action. (Boulluec et al. 2013). Also, diffracted waves and reflected waves due to the offshore wind turbine motions will reach the tank walls and then be reflected back to the model. In this way, a transverse wave system will gradually be developed, and the tank wall interference effects can have a very important effect on the experimental results (Steen 2014, Zhao et al. 1988). Also, the time between two consecutive test cases should be long enough to ensure an acceptable quiescence of water. The Type B uncertainty should be estimated by the past experiences.

3.7 Other sources of uncertainties

3.7.1 Scaling effects

For offshore wind turbines, aerodynamic and hydrodynamic loads can be of equal importance when estimating its dynamic response. While for hydrodynamic loads Froude scaling is usually adopted, the aerodynamic forces should be scaled according to Reynolds scaling. The two dimensionless ratios cannot be satisfied simultaneously, and usually offshore wind turbine models are Froude scaled. Therefore, the mismatch of Reynolds number is a source of uncertainty for aerodynamic loads that should be considered in the design of the test setup. See

ITTC Procedure 7.5-02-07-03.8, “Model Tests for Offshore Wind Turbines” (ITTC, 2017c) for different approaches of modelling the wind turbine. E.g., for performance modelling, the blades are redesigned to provide the same thrust and torque characteristics in the low Reynolds number regime as in full scale. Uncertainty analysis should be conducted on the redesigned blades to determine the degree to which the target wind load characteristics have been achieved and to allow this effect to be included in an analysis of the overall model test.

Additional uncertainty sources due to the scaling, in common with other offshore structures, are viscous effects on the hull (e.g., slender parts, appendages) and mooring lines. See also Qiu et al. (2014).

3.7.2 Human factors

Human factors can be classified as error rather than uncertainty sources. See, e.g., Qiu et al. (2014) for further details.

4. EXAMPLE OF UNCERTAINTY ANALYSIS TO OFFSHORE WIND TURBINE MODEL TEST

The following example is based on the article: “Dynamic response of a monopile wind turbine in waves: Experimental uncertainty analysis for validation of numerical tools” (Bachynski et al., 2019).

4.1 Experimental model

The prototype design corresponds to the NREL 5MW reference wind turbine (Jonkman et al., 2009), supported by the offshore tower developed in OC3 Phase III (Jonkman, 2010) and a 7 m diameter monopile, with the OC3 Phase II soil stiffness parameters (Jonkman and Musial, 2010). The monopile thickness is 60 mm and the transition from monopile to tower occurs at 10 m above the waterline.

Table 2: Key model particulars, compared to the design prototype and to the OC3 Phase II monopile (Jonkman and Musial, 2010). All values in full scale. Note that the OC3 Phase II monopile is in 20 m water depth, compared to the present model in 30 m water depth.

	Model Tests	Prototype	OC3 Phase II Monopile
Diameter (wetted section of monopole) [m]	7.0	7.0	6.0
Tower base diameter (10 m above waterline) [m]	6.5	6.5	6.0
Tower top diameter [m]	3.87	3.87	3.87
RNA mass [kg]	3.36×10^5	3.50×10^5	3.50×10^5
RNA Ixx about RNA CoG [kg m^2]	7.14×10^7	4.00×10^7	4.00×10^7
RNA Iyy about RNA CoG [kg m^2]	7.14×10^7	3.07×10^7	3.07×10^7
RNA Izz about RNA CoG [kg m^2]	9.51×10^7	2.44×10^7	2.44×10^7
Monopile penetration depth (below seabed) [m]	-	46	30

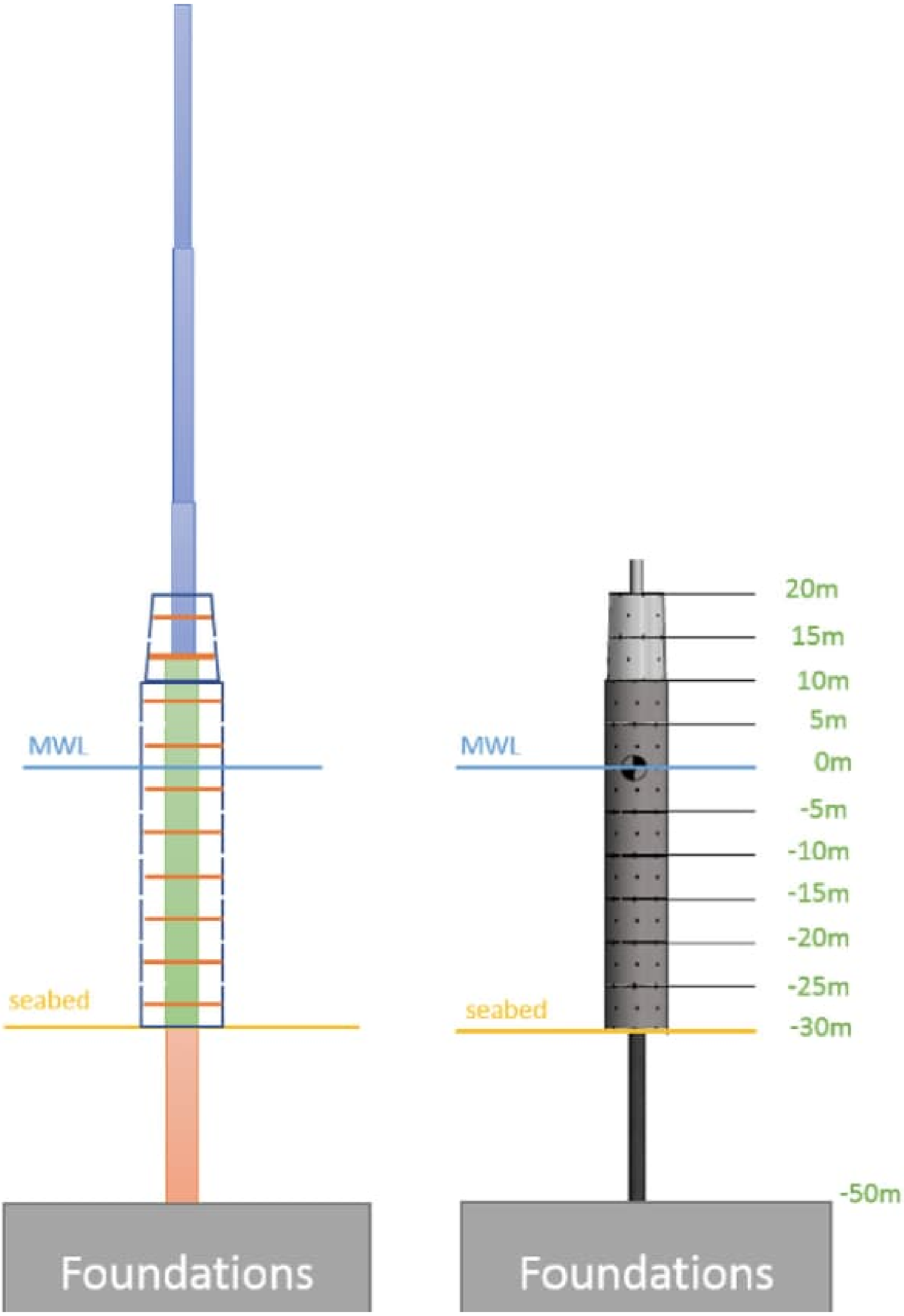

Figure 3: Sketch of the monopile model, without (left) and with (right) outer shells

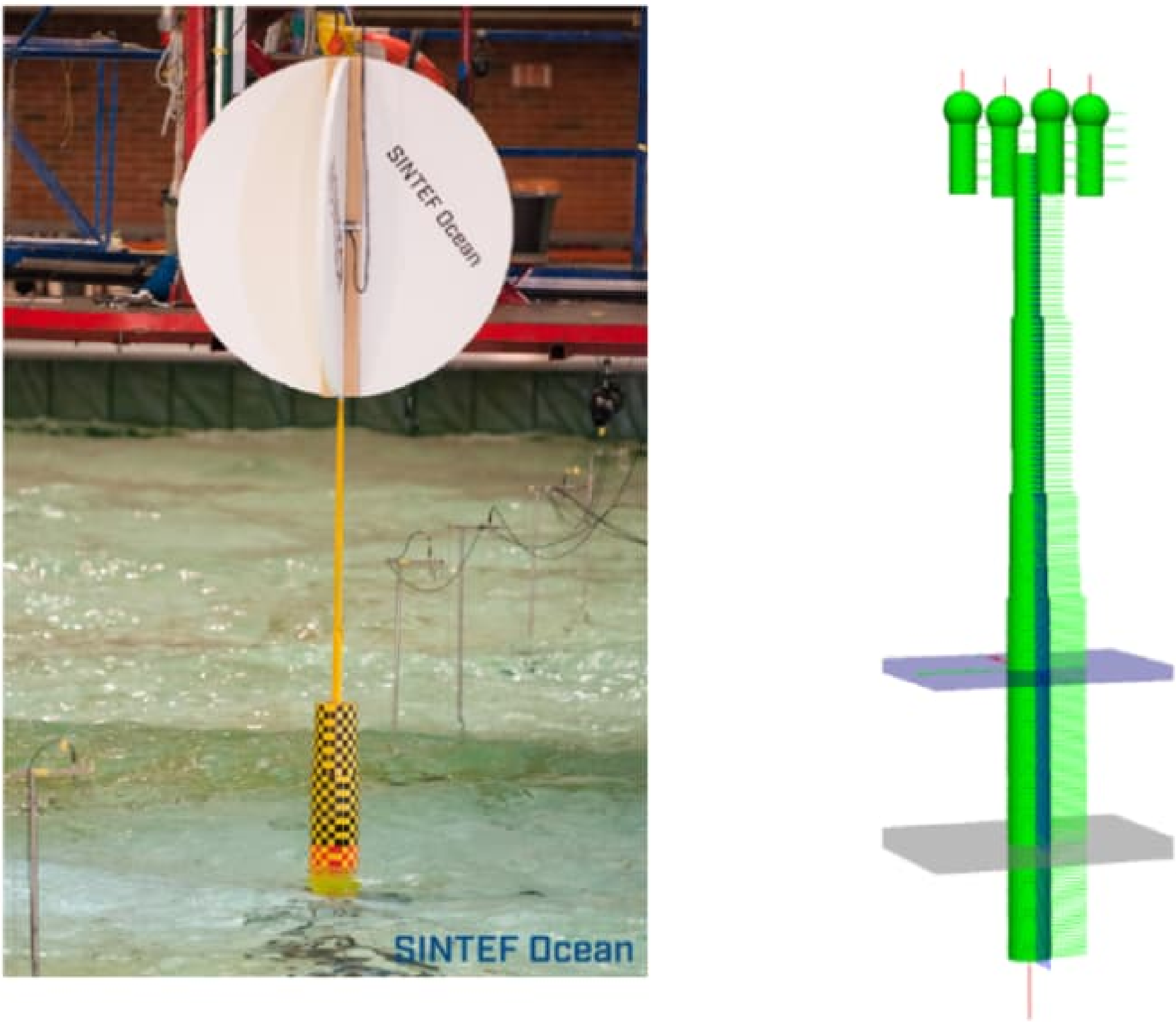

Figure 4: Left: photograph of the model installed in the wave basin, highlighting the drag disk. Right: numerical model in SIMA, where the four upper lines represent the drag disk. Transition from red to black checkerboard in the picture to the left indicates the calm water free surface

The model tests were carried out at a scale of 1:40 in the Ocean Basin at SINTEF Ocean (Figure 4). Froude scaling (including the difference between the freshwater density in the model tests and sea water density at full scale) was applied in order to scale the model test results.

4.2 Regular Wave Test

As shown in Table 3 nine regular waves were tested, with periods (T) ranging from 6 to 14 seconds. The steepness-value was considered (approximately 1/30). The Keulegan-Carpenter

(KC) number, defined in Equation (4), for all the considered tests is quite low. For the smallest waves (KC < 1.25), no flow separation is expected (Sarpkaya and Isaacson, 1981), and for KC up to 5.0, the added mass coefficient is not expected to vary significantly (DNV, 2010). In Table 3, the KC number for regular waves is calculated, based on the maximum velocity according to linear theory by Equation (4):

$$KC = \frac{U_{max}T}{D} = \frac{\pi H_1}{\tanh(kh)D} \tag{4}$$

where U_{max} is the maximum water particle velocity, perpendicular to the monopile axis, at water surface level, T is the wave period, H is the regular wave height, k is the wave number, h is the water depth, and D is the diameter of the monopile (characteristic length).

Table 3: Regular wave tests (full scale).

H [m]	1.9	2.6	3.3	4.2	5.2	6.3	7.5	8.8	10.2
T [s]	6.0	7.0	8.0	9.0	10.0	11.0	12.0	13.0	14.0
KC	0.85	1.18	1.54	2.04	2.65	3.39	4.27	5.31	6.50

4.3 Bending moment RAOs

The bending moment transfer function $R(\omega)$, denoted as the response amplitude operator (RAO) of the bending moment at z = −28.5 m, for the first harmonic of the primary wave frequency for wave periods 6 s, is defined in Equation (3):

$$R(\omega) = My_1 / \eta_1 \tag{3}$$

Where My_1 is the amplitude of the first harmonic bending moment, and η_1 is the amplitude of the first harmonic wave.

4.4 Type A Uncertainty

Type A uncertainties are evaluation of uncertainty by the statistical analysis of a series of observations (JCGM (2008a). This type of uncertainty is also commonly known as the precision uncertainty of the test. Repeatability is assessed directly from the experimental results.

4.4.1 Waves

Assessing the repeatability of the RAO is challenging for several reasons. The generation of regular waves in relatively shallow water can be challenging due to the depth variations and reflections, standing waves, and parasitic waves in the basin.

There were 13 standing probes (present during both the calibration and the tests with the model) and 23 probes along a wave harp (a set of tightly spaced wave probes aligned with the wave propagation direction, with a distance of 6 m between each probe and connected to a single support), which was only present during wave calibration. The wave harp is shown in Figure 5.

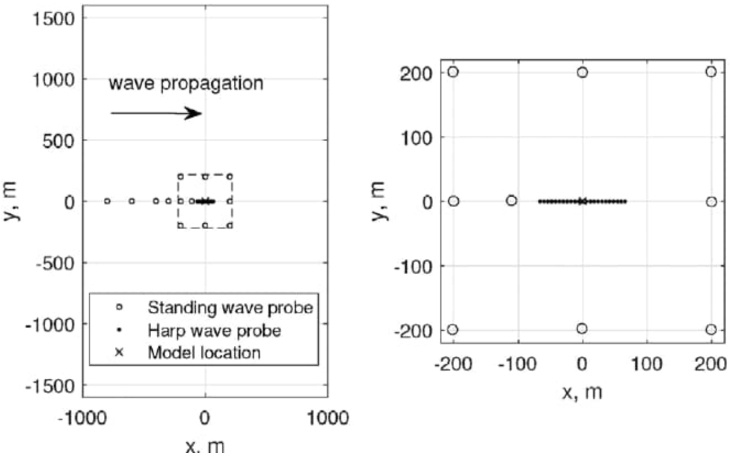

Figure 5: Wave probe layout during calibration of long-crested waves. Right: zoom near the model, showing the tightly spaced wave probes in the harp (a set of tightly-spaced wave probes aligned with the wave propagation direction)

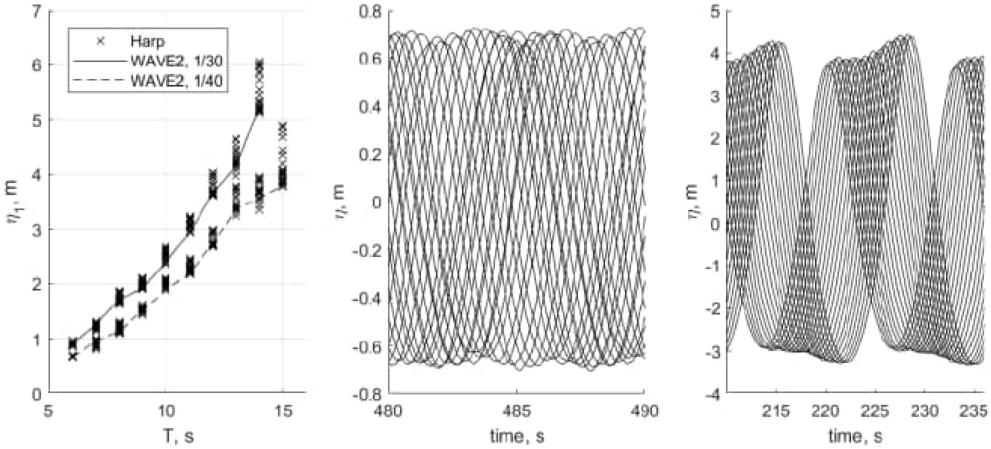

Figure 6: Variations in regular wave amplitude along the wave harp. Left: amplitude of the first harmonic of the wave along the harp, where WAVE2 shows the value at the model location. Note that the indicated steepness 1/30 and 1/40 are approximate. Middle: time series of wave elevation along the harp (T = 6 s, lower steepness). Right: time series of wave elevation along the harp (T = 13 s, lower steepness)

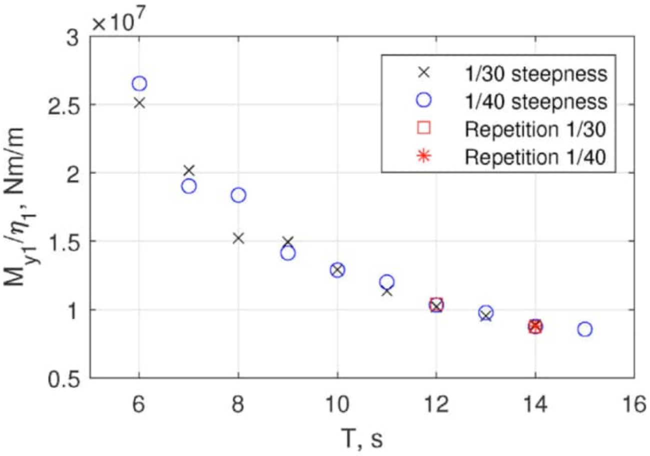

Figure 7: Experimental bending moment (at z = - 28:5 m) RAO results, highlighting the repeatability and the differences in results for different wave steepness

There are notable differences in the amplitude of the first harmonic of the wave, especially for the longest waves (Figure 6).

The wave amplitude at a given location along the harp deviates up to 18 % compared to the mean amplitude, and the coefficient of variation ranges from 3 to 9 % depending on the wave period.

4.4.2 Assessment of Type A standard uncertainty

Type A standard uncertainty of a response which is measured repeatedly is found from Equation (5):

$$s_R = \frac{s_x}{\sqrt{N-1}} \tag{5}$$

where s_x is the standard deviation of the measured quantity over N repeated tests.

Please notice that, in Equation (5), the denominator *N-1* is used rather than *N*, as in Equation (3), due to the Bessel's correction, i.e. Equation (3) can only be used for the population variance, while in general, at practical level, only a sample of the whole population is available during a test, and Equation (5) is used to calculate the sample variance.

There is a good agreement in the first harmonic RAO for longer waves as shown in Figure 7. The repeated tests also showed good agreement (within 2 %) for the first harmonic. The discrepancies between the results for the different wave steepness were large, but the repeatability of each condition was within 5 %.

Type A standard uncertainty of bending moment transfer function was:

$$s_R = 0.354\text{E+05 Nm/m}$$

4.5 Type B Uncertainty

Type B uncertainties are the evaluation of uncertainty by means other than statistical analysis (JCGM (2008a)). These are also commonly known as bias uncertainties.

4.5.1 Temperature and Density

The temperature was measured to be 16 ^{0}C , and the temperature variations during the model tests were ±0.07 ^{0}C. Based on the manufacturer data, the temperature error is 0.03 % per ^{0}C: considering temperature variations of ±0.07 ^{0}C, the temperature contribution to the Type B standard uncertainty is negligible compared to the previously described contributions. By applying the method outlined in the water properties ITTC Procedure 7.5-02-01-03, “Density and Viscosity of Water”, the density (ρ) is 999.072 kg/m^3 and the corresponding Type B standard Uncertainty is 0.0306 kg/m^3.

4.5.2 Wave gauges

The wave gauges have a sensitivity of 2 % / ^{0}C. Temperature effects had a relatively small contribution to the Type B uncertainty for the wave gauges.

4.5.3 Strain gauges

Calibration of the strain gauges is carried out by applying a known moment (via a hanging weight attached through a pulley at a given height). We estimated the Type B standard uncertainty by considering ±2 mm model scale error in height and ±5 ^{0}C standard uncertainty in orientation of the load applied for calibration.

4.5.4 Geometry and Inertia of Experimental Model

Possible Type B uncertainties in manufacture of the experimental model are estimated in Table 4 and propagate to the responses of interest using a simple semi-analytical model.

Table 4: Estimated Type B uncertainties. All values given in full scale

Parameter	Type B standard uncertainty
Measured wave elevation	± 3 %
Water depth	± 0.4 m
Mass distribution	± 10 % locally
Inner core dimensions	± 4 mm
Outer core dimensions	± 6 cm
Strain	± 0.5 %
Acceleration	Orientation $\pm 2.5^\circ$, location 0.12 m

4.5.5 Bending moment RAO

The uncertainty in these response metrics, i.e. bending moment RAO, will depend on the uncertainty in the incoming waves, the model itself (i.e. geometry, stiffness, mass distribution), and the measured response (bending moment) as in Table 5.

Table 5: Independent input variables for semi-analytical analysis

Input variable	Symbol	Comments
Mass distribution	m	Affects modal parameters. Uniform relative variation 10 %
Stiffness distribution	EI	Affects modal parameters. Uniform relative variation 4 %
Modal damping	b_i or ζ	Varied for all five modes simultaneously 20 %
Outer diameter	D	Only affects wave loads, 6 cm

Water depth	h	Affects modal parameters and wave loads, 0.4 m
Regular wave period	$\frac{2\pi}{\omega}$	Affects wave loads, 0.05 s

4.6 Simplified semi-analytical uncertainty propagation

A simplified model is used to propagate Type B uncertainties in the properties of the physical model and in the incoming waves to the bending moment response. This linearized model is obtained by combining a 5-mode structural response model with linear wave loads. The structural response model takes the form of the decoupled ordinary differential equations in Equation (6) through (9), where $\overline{m_\iota}$ is the modal mass, $\overline{b_\iota}$ is the modal damping, $\overline{k_\iota}$ is the modal stiffness, $\overline{F_\iota}$ is the modal force, and y_i is the modal response.

$$\overline{m_\iota}\ddot{y}_\iota + \overline{b_\iota}\dot{y}_\iota + \overline{k_\iota}y_i = \overline{F_\iota}, i = 1, \dots, 5 \tag{6}$$

$$\overline{m_\iota} = \int_{z_{low}}^{z_{top}} m(z)(\varphi_i(z))^2\, dz + \sum M_j\, (\varphi_i(z_j))^2 + \sum I_j\, (\varphi_{i,z}(z_j))^2 \tag{7}$$

$$\overline{k_\iota} = \int_{z_{low}}^{z_{top}} EI(z)(\varphi_{i,zz}(z))^2\, dz \tag{8}$$

$$\overline{b_\iota} = 2\overline{m_\iota}\,\omega_{0,i}\,\zeta = 2\zeta\sqrt{\overline{k_\iota}\,\overline{m_\iota}} \tag{9}$$

The undamped natural frequencies obtained from the estimated modal mass and stiffness were found to be within 5 % of those from the eigenvalue analysis. For simplicity, the modal damping is chosen to give the same damping ratio in all five modes. Based on the decay tests, ζ = 0.5 % critical damping is chosen.

In the modal response model, the viscous drag term of the Morison equation was not considered due to the relatively low KC number of the experiments as in Table 3. Then the Morison inertia load takes the form as in Equation (10):

$$\overline{F_\iota} = \int_{-h}^{0} \varphi_i(z)\rho(C_a + 1)\pi\frac{D^2}{4} a dz \tag{10}$$

with a for regular waves with amplitude η_a and frequency $\omega = 2\pi/T$ in water depth h given by Equation (11):

$$\mathrm{a} = \omega^2\eta_a \frac{\cosh(k(z+h))}{\sinh(kh)}\cos\omega t \tag{11}$$

According to this simple semi-analytical model, the first response metric, the first harmonic bending moment RAO at z_j = - 28.5 m, is given by Equation (12).

$$|H(\omega)| = \frac{\left|M|_{z_j}\right|}{|\eta_a|} = \sum_{i=1}^{n} EI(z_j)\,\varphi_{i,zz}(z_j) * \frac{\int_{-h}^{0}(C_a+1)\pi\frac{D^2}{4}\rho\omega^2\frac{\cosh(k(z+h))}{\sinh(kh)}\varphi_i(z)dz}{\overline{k_\iota}\sqrt{((1-\beta_i^2\,)^2+(2\,\zeta_i\beta_i)^2}} \tag{12}$$

In Equation (13), β_i is the frequency ratio for each mode.

$$\beta_i = \frac{\omega}{\omega_i} = \frac{\omega\sqrt{\overline{m_\iota}}}{\sqrt{\overline{k_\iota}}} \tag{13}$$

4.7 Total Type B Uncertainty

To compute the total Type B standard uncertainty in the measured response u_R, we combine the effects of the inputs in Table 4 with the effects of the estimated bias uncertainties in the wave elevation and bending moment measurements.

Considering a result R which depends on L independent variables x_i, the sensitivity index θ_i is given by Equation (14):

$$\theta_i = \frac{\partial R}{\partial x_i}, \quad i = 1, 2, \ldots, L \tag{14}$$

and evaluated at either mean or nominal values of the result.

The standard uncertainty in the result due to the Type B uncertainties is obtained by the square root of the sum of squares (RSS) of the contributions from all of the independent variables by Equation (15):

$$u_R = \pm\sqrt{\sum_{i=1}^{L}(\theta_i u_{x_i})^2} \tag{15}$$

where u_{xi} is the best estimate of the standard uncertainty in the independent variable.

The most important components of Type B standard uncertainty of bending moment transfer function $R(\omega)$ at T = 6 s are the wave elevation, mass, and diameter as in Equation (16):

$$R(\omega) = RAO = {}^{M_y}/_{\eta_y} =$$

$$f\left(m, EI, \zeta, D, h, T, M_y, \eta_a\right) \tag{16}$$

A calculation in wave period, T = 6 s is made by Equation (17), referring to the values in Table 6.

Table 6: Sensitivity indexes and independent variable uncertainty values

Variable x_i	$\boldsymbol{\theta_{x_i}}$	Units for $\boldsymbol{\theta_{x_i}}$	$\boldsymbol{u_{x_i}}$	Units for $\boldsymbol{u_{x_i}}$	$\boldsymbol{\theta_{x_i} u_{x_i}}$	Units for $\boldsymbol{\theta_{x_i} u_{x_i}}$
M	2.55E+03	Nm/(mkg/m)	203.5	kg/m	5.19E+05	Nm/m
EI	4.70E-05	Nm/(mNm^2)	5.60E+09	Nm^2	2.63E+05	Nm/m
ζ	7.30E+05	Nm/m	0.001	-	7.30E+02	Nm/m
D	7.03E+06	Nm/m^2	0.06	m	4.22E+05	Nm/m
h	2.74E+04	Nm/m^2	0.4	m	1.10E+04	Nm/m
T,	9.12E+06	Nm/(ms)	0.05	s	4.56E+05	Nm/m
M_y	1.05E+00	Nm/(mNm)	116,840.5	Nm	1.23E+05	Nm/m
η_a	2.51E+07	Nm/m^2	0.0285	m	7.16E+05	Nm/m

$$u_R = \sqrt{(\theta_m u_m)^2 + (\theta_{EI} u_{EI})^2 + (\theta_\zeta u_\zeta)^2 + (\theta_D u_D)^2 + (\theta_h u_h)^2 + (\theta_T u_T)^2 + (\theta_{M_y} u_{M_y})^2 + (\theta_{\eta_a} u_{\eta_a})^2} = 1.12E+06\ Nm/m \tag{17}$$

As shown in Equation (14), Type B uncertainties are generally larger than Type A uncertainty. The Type B uncertainties generally decrease for longer wave periods, and the importance of the mass distribution becomes smaller for longer waves. This is as expected, since the monopile response becomes increasingly stiffness-dominated for long wave periods.

4.8 Total Uncertainty

The total uncertainty is a combination of both the known Type A and Type B uncertainties, (Type A standard uncertainty s_R and Type B standard uncertainty u_R). To combine Type A and Type B standard uncertainties, the square root of the sum of squares is again used in Equation (18):

$$u_c = \sqrt{{u_R}^2 + {s_R}^2} \quad (18)$$

where $u_c = 1.12\,\mathrm{E}+06$ Nm/m, u_R = 1.12 E+06 Nm/m, and s_R = 3.54 E+04 Nm/m.

4.9 Conclusions

The uncertainty analysis suggests that Type A uncertainties (estimated through repetition tests) are of minor importance compared to Type B uncertainties (estimated through a simplified analytical uncertainty propagation) for the estimation of RAOs. Based on a somewhat conservative estimate - local variation applied as a global variation - the mass and stiffness of the model itself were found to be important contributors to Type B uncertainty. The wave elevation and model diameter, where Type B uncertainties were estimated more realistically, were also seen to be important.

5. REFERENCES

Azcona, J., Bredmose, H., Campagnolo, F., Manjock, A., Pereira, R., and Sander, F., 2014, “Methods for performing scale-tests for method and model validation”, Technical report, INNWIND.EU Deliverable D4.22.

Bachynski, E.E., Thys, M., Sauder, T., Chabaud, V., and Saether, L.O., 2016, “Real-time hybrid model testing of a braceless semi-submersible wind turbine. Part II: Experimental results”, Proc. 35th Int. Conf. on Ocean, Offshore and Arctic Engineering OMAE 2016, Busan, Korea.

Bachynski E. E., Thys, M., Delhayec V., 2019, “Dynamic response of a monopile wind turbine in waves: Experimental uncertainty analysis for validation of numerical tools”, Applied Ocean Research, Volume 89, pp 96-114.

Berthelsen, P.A., Bachynski, E. E., Karimirad, M., Thys, M., 2016, “Real-time hybrid model testing of a braceless semi-submersible wind turbine. Part III: Calibration of a numerical model”, Proc. 35th Int. Conf. on Ocean, Offshore and Arctic Engineering OMAE 2016, Busan, Korea.

Boulluec, M.L., Ohana J., Martin, A., Houmard A., 2013, “Tank testing of a new concept of floating offshore wind turbine”, Proc. 32nd Int. Conf. on Ocean, Offshore and Arctic Engineering OMAE 2013, Nantes, France.

Couto, P.R.G, Damasceno, J.C., and de Oliveira, S.P., 2013, “Monte Carlo Simulations Applied to Uncertainty in Measurement”, in Theory and Applications of Monte Carlo Simulations, InTech (2013): Chap. 2, pp. 27–51. V. Chan (Ed.).

Det Norske Veritas, 2010, Environmental conditions and environmental loads, Tech. Rep. DNV-RP-C205.

Gueydon, S. 2016, "Aerodynamic Damping on a Semisubmersible Floating Foundation for Wind Turbines", Energy Procedia, Volume 94, pp 367-378, ISSN 1876-6102.

Gupta, S. and Leishman, J., 2005. “Comparison of momentum and vortex methods for the aerodynamic analysis of wind turbines”, 43rd AIAA Aerospace Sciences Meeting and Exhibit (p. 594).

ITTC, 2011, “Recommended procedures and guidelines: Seakeeping experiments”, ITTC Procedure 7.5-02-07-02.1, Revision 04, 25th International Towing Tank Conference.

ITTC, 2014a, "Guide to the Expression of Uncertainty in Experimental Hydrodynamics", ITTC Procedure 7.5-02-01-01, Revision 02, 27th International Towing Tank Conference.

ITTC, 2014b, "General Guideline for Uncertainty Analysis in Resistance Tests", ITTC Procedures 7.5-02-02-02, Revision 02, 27th International Towing Tank Conference.

ITTC, 2017a, "Guideline to Practical Implementation of Uncertainty Analysis", ITTC Procedures 7.5-02-01-07, Revision 00, 28th International Towing Tank Conference.

ITTC, 2017b, “Floating Offshore Platform Experiments”, ITTC Recommended Procedures 7.5-02-07-03.1, Revision 02, 28th International Towing Tank Conference.

ITTC, 2017c, “Model Tests for Offshore Wind Turbines”, ITTC Recommended Procedures 7.5-02-07-03.8, Revision 01, 28th International Towing Tank Conference.

JCGM, 2008a, "Evaluation of measurement data – Guide to the expression of uncertainty in measurement", JGCM 100:2008 GUM 1995 with minor corrections, Joint Committee for Guides in Metrology, Bureau International des Poids Mesures (BIPM), Sèvres, France.

JCGM, 2008b, "Evaluation of measurement data – Supplement 1 to the Guide to the expression of Uncertainty in measurement – Propagation of distributions using a Monte Carlo method", JGCM 101:2008, Joint Committee for Guides in Metrology, Bureau International des Poids Mesures (BIPM), Sèvres, France.

Jonkman J., 2007, “Dynamics Modeling and Loads Analysis of an Offshore Floating Wind Turbine,” Technical Report NREL/TP-500-41958, (November 2007).

Jonkman J., Butterfield S., Musial W., Scott G., 2009, Definition of a 5-MW reference wind turbine for offshore system development, Tech. Rep. NREL/TP-500-38060, National Renewable Energy Laboratory (February 2009).

Jonkman J., 2010, Definition of the floating system for Phase IV of OC3, Tech. Rep. NREL/TLP-500-47535.

Jonkman J, Musial W., 2010, Offshore code comparison collaboration (OC3) for IEA Wind Task 23 offshore wind technology and deployment, Tech. Rep. NREL/TP-5000-48191, National Renewable Energy Laboratory.

Qiu, W., Sales Jr, J., Lee, D., Lie, H., Magarovskii, V., Mikami, T., Rousset, J.-M., Sphaier, S., Tao, L., Wang, X., 2014, "Uncertainties related to predictions of loads and responses for ocean and offshore structures", Ocean Engineering, Vol 86, pp. 58 – 67.

Robertson, A.N., 2017. “Uncertainty analysis of OC5-DeepCwind floating semisubmersible offshore wind test campaign”, (No. NREL/CP-5000-68035). National Renewable Energy Lab.(NREL), Golden, CO (United States).

Sauder, T., Chabaud, V., Thys, M., Bachynski, E. E., and Saether, L.O., 2016, “Real-time hybrid model testing of a braceless semi-submersible wind turbine. Part I: The hybrid approach”, Proc. 35th Int. Conf. on Ocean, Offshore and Arctic Engineering OMAE 2016, Busan, Korea.

Sarpkaya T., Isaacson M., 1981, Mechanics of wave forces on offshore structures, Van Nostrand Reinhold.

Steen, S., 2014, “Experimental methods in Marine Hydrodynamics”, Lecture note, NTNU, Trondheim, Norway.

Urban A. M., Guanche R., 2019, "Wind turbine aerodynamics scale-modeling for floating offshore wind platform testing", Journal of Wind Engineering & Industrial Aerodynamics 186 (2019) 49–57.

Zhao, R., Faltinsen, O.M., Krokstad, J., Aanesland, V., 1988, “Wave-current interaction effects on large-volume structures”, BOSS ’88, Trondheim, Norway.